SUPPLEMENTAL MATERIAL

Supplemental Methods

Plasmid, antibodies and reagents

The following plasmids were used for whole experiments: Human *KCNQ1* and *KCNE1* in pcDNA3.1(+) vector (gifts from Dr. Robert S. Kass, Columbia University), GFP-tagged human *KCNQ1* in pEGFP-N2 (kindly provided from Dr. Gildas Loussouarn, IRT UN, France)[1] human *KCNQ1* in modified pIRES2 vector in containing the fluorescent protein cDNA of DsRed-MST instead of GFP (generously provided by Dr. Alfred George, Vanderbilt University),[2] pcDNA3.1(+) vector (Invitrogen) and pEGFP-N1 vector (Clontech). Mutations were introduced into *KCNQ1* and GFP-tagged *KCNQ1* using the PCR based site direct mutagenesis was performed using PFU ultra DNA polymerase (Agilent Technologies).[3] Construct sequences were confirmed by DNA sequencing at Functional Genomics Center, University of Rochester Medical Center.

The following antibodies were used for immunoblot: anti-*KCNQ1* antibody (goat polyclonal IgG, Santa Cruz Biotechnology) raised against the peptide mapping at the C-terminus of *KCNQ1* of human origin, anti-β-actin antibody (mouse monoclonal IgG, GenScript USA), IRDye800-conjugated anti-goat antibody (Rockland Immunochemicals), and Alexa Fluor® 680 goat anti-mouse antibody (Invitrogen).

All reagents were purchased from Sigma-Aldrich Corporation unless otherwise indicated. Adenylyl cyclase activator, forskolin was dissolved in Dimethyl sulfoxide (DMSO) to make 25mM stock and stored at -20°C.

Cell culture and transfection

HEK293T cells (generously provided from Dr. Keigi Fujiwara, University of Rochester) were maintained in high glucose (4.5 g/L) Dulbecco's modified Eagle's medium (Mediatech) supplemented with 10% fetal bovine serum (Equitech-Bio) and 1% L-glutamax (Invitrogen) in a humidified incubator with 5% CO_2.[3-4] Cells were transfected with FUGENE-HD transfection regents (Roche), re-plated 24 hours after transfection by using Acutase (Innovative Cell Technologies) and used for experiments 48 hours after transfection.

Western blot analysis

Expression of wild-type (WT)- and mutant-*KCNQ1* subunits were confirmed by Western blot. Whole cell lysates were prepared from HEK293T cells, separated by 10% SDS-PAGE, transferred to nitrocellulose membrane (Bio-Rad) and incubated with primary antibodies, followed by incubation with fluorescence-conjugated secondary antibodies.[5] Immunoreactive bands were visualized by Odyssey Infrared Imaging System (LI-COR Biotechnology, Lincoln NE). Densitometric analyses of immunoblots were performed with NIH Image J software. The expression of β-actin was used to control for protein loading in each condition. Mutant band intensity were normalized to wild-type intensity in each blot.

Analysis of co-transfection efficiency

GFP-tagged mutant constructs and wild-type subunits in a vector that can expressed DsRed fluorecent protein in addition to the WT subunit were used (Supplementary figure 1S top panel). Co-expression of WT- and mutant-*KCNQ1* subunits were observed using laser scanning confocal microscope (Fluoview FV1000, Olympus) with images obtained using

Fluoview software (FV10-ASW ver2.1c, Olympus) in live cells at room temperature in Tyrode's solution.[6] The composition of Tyrode's solution was as follows (mM): NaCl, 136.9; KCl, 5.4; $CaCl_2$, 2; $MgCl_2$, 0.5; NaH_2PO_4, 0.33; HEPES, 5; glucose, 5, pH 7.40 adjusted with NaOH. HEK293T cells were transfected with GFP-tagged mutant *KCNQ1*, WT-*KCNQ1* in pIRES2- DsRed-MST vector and *KCNE1* at the ratio of 0.5: 0.5: 1.

In order to study the heterozygous mutant channel, expression of both wild-type and mutant channel subunits in the same cells is necessary. To address whether co-transfection of wild-type and mutant subunits in HEK293 cells yielded expression of both subunits, we used fluorescence tagged constructs (Top panel A). A typical group of cells showing mutant and wild type expression is depicted at the bottom of panel A. In panel B, green (mutant expressing) and red (wild-type expressing) cells were counted and separated into three groups: 1) only WT subunit-expressed cells despite co-transfection of the mutant subunit (only red fluorescence from DsRed), 2) only mutant subunit-expressed cells despite co-transfetion of wild-type subunit (only green fluorescence from EGFP) and 3) the desired combination of WT- and mutant subunit-coexpressed cells (both green and red fluorescence). For 85-95% of cells, WT and mutant-*KCNQ1* were co-expressed, suggesting that this transfection protocol leads to expression of both subunits in the same cells and the heterozygous expression of the channel subunits (Supplementary Figure 1S bottom panel). Using electrophysiology measurements (see next section for details), we determined that for all heterozygous mutant channels transfected, in about 10% of total cells patched, fast current activation characteristic of *KCNQ1* expressed alone without *KCNE1* subunits [7] was

observed. These cells were not used for determination of channel regulation. This number is consistent with a high co-transfection efficiency of the KCNE1 subunit.

Electrophysiology

Wild type *KCNQ1:KCNE1* DNA were expressed in HEK293T cells either at a ratio of 1:1 or 0.5:1, mimicking the haploinsufficient phenotype. Empty plasmid was added to maintain total DNA concentration constant. Each mutant *KCNQ1* plasmid was co-transfected with WT *KCNQ1* and *KCNE1* at the ratio of 0.5 μg mutant *KCNQ1*:0.5 μg WT-*KCNQ1*:1μg *KCNE1* to yield heterozygous mutant channel expressed. Cells were also co-transfected with low amounts of pEGFP-N1 (0.2 μg) to allow identification of transfected cells using fluorescence. Selection of bright green cells, expressing high concentration of pEGFP, are expected to have higher concentration of the other transfected plasmids, decreasing the inherent variability of the subunit expression levels. In a small percentage of cells (about 10% of total cells patched for all mutants), fast current activation characteristic of *KCNQ1* expressed alone without *KCNE1* subunits was observed. These cells were not used for determination of channel regulation.

K^+ currents were measured using an Axon 200B amplifier (Axon Instruments) and conventional whole cell patch clamp techniques. The tip resistances of glass pipettes were of 2–6 MΩ. Voltage-clamp protocols and data acquisition and analyses were performed using Clampex software (Axon Instruments). The voltage drop across the access resistance was compensated >70%. Whole cell currents were recorded using a low-pass filter with an 1 kHz cutoff and sampled at 2–5 kHz.

The composition of the extracellular solution for the I_{Ks} measurements was (in mmol/L): 145 NaCl, 5.4 KCl, 1. $MgCl_2$, 1.8 $CaCl_2$, 10 HEPES, 10 glucose (pH 7.40 adjusted with NaOH). The composition of the pipette solution was (in mmol/L): 130 K-aspartate, 11 EGTA, 1. $MgCl_2$, 1 $CaCl_2$, 10 HEPES, 5 K-ATP (pH 7.20 adjusted with KOH). Cell-plated glass cover slides were placed on recording chamber (Warner Instruments) and continuously perfused with extracellular solution. All experiments were performed at room temperature (≅ 22°C).

Currents time course was measured using a 4-sec depolarization pulse to +20 mV from a holding potential of -80 mV, followed by a 2-sec pulse to -20mV repeated every 10 sec. Current-voltage (I-V) relationships were obtained using a series of test pulses between -40 mV and +120 mV in 10-mV increments before and after forskolin treatment. Baseline mutant current was compared to the current measured from haploinsufficient control channel (0.5 ng WT-*KCNQ1*: 1ng *KCNE1*). The time course of current regulation by forskolin for channels formed by mutant subunits co-expressed with WT subunits was normalized to the changes measured in the absence of forskolin application over the same time course. The time course of current regulation by forskolin in WT channels was measured from cells transfected with 1 μg WT-*KCNQ1* and 1 μg *KCNE1*.

Statistics

One-way ANOVA followed by Tukey Post Hoc test was applied for the assessment of statistical significance for multiple group comparison by using SPSS Statistics ver 17 (IBM). Unpaired Student T-test was used for two group comparison. The significance was set at $p< 0.05$.

Supplemental Tables

Table 1S. Distribution of Mutation Location and Type in LQT1 patients

Missense									Nonmissense		
C/N terminal			Membrane spanning			Cytoplasmic loops					
Codon	**n (%)**	**Dominant Negative***	**Codon**	**n (%)**	**Dominant Negative***	**Codon**	**n (%)**	**Dominant Negative***	**Type**	**n (%)**	**Dominant Negative***
All	172 (20)	-	All	376 (44)	-	All	125 (15)	-	All	187 (22)	-
R591H	19 (11)	No [3]	G168R	67 (18)	Yes [3†]	V254M	62 (50)	Yes [3†]	A344A/sp	41 (22)	No‡
H363N	17 (10)	Unknown	G269S	41 (11)	Yes [3]	Y184S	18 (14)	Yes [3]	Q530X	25 (13)	No‡
R366W	15 (9)	Unknown	G269D	24 (6)	Yes [8]	R243C	13 (10)	Yes [3†]	R518X	19 (10)	No‡
R594Q	14 (8)	No [3]	L266P	24 (6)	Yes [3]	A178P	5 (4)	Yes [9]	K598K/sp	17 (9)	No‡
D611Y	10 (6)	No [3]	A341V	22 (6)	Yes [3]	R259L	5 (4)	Unknown	448 insG	11 (6)	No‡
K393N	10 (6)	Unknown	G314S	19 (5)	Yes [3]	G189R	4 (3)	Yes †	delF340	9 (5)	No‡
S373P	8 (5)	Unknown	A344V	18 (5)	Unknown	R190Q	4 (3)	Yes †	IVS +5 G>A	8 (4)	Unknown
G568R	7 (4)	Unknown	T312I	17 (5)	Yes [3†]	D242N	3 (2)	Unknown	IVS7 +5 G>A	8 (4)	Unknown
I567S	7 (4)	Unknown	W305S	16 (4)	Yes [3]	G189E	2 (2)	Unknown	L191fs/90	8 (4)	No‡
R555C	7 (4)	Yes †	S225L	15 (4)	Yes [3†]	R174H	2 (2)	Unknown	P400fs/62	7 (4)	No‡
V524G	6 (3)	Unknown	S349W	15 (4)	Yes [3]	R259C	3 (2)	Yes [10]	Y171X	7 (4)	No‡
R397W	5 (3)	Unknown	E160K	12 (3)	unknown	A178T	1 (1)	Unknown	S349X	6 (3)	No‡
R591C	5 (3)	Unknown	A341E	10 (3)	Yes [3]	D242Y	1 (1)	Unknown	intron2,-2 G/A	4 (2)	Unknown
S546L	5 (3)	Unknown	L273F	10 (3)	Yes [9]	R190W	1 (1)	Unknown	S571fs/20	3 (2)	No‡
R562S	4 (2)	Unknown	Y315C	10 (3)	Yes [3]	R243S	1 (1)	Unknown	639+5G>A	2 (1)	Unknown
A590T	3 (2)	Unknown	G325R	8 (2)	Unknown				A150fs/133	2 (1)	No‡
D455Y	3 (2)	Unknown	S277L	8 (2)	Unknown				A636fs/28	2 (1)	No‡
I517T	3 (2)	Unknown	D317G	5 (1)	Unknown				IVS2 +1 G>A	2 (1)	Unknown
K557E	3 (2)	Unknown	L353P	4 (1)	Unknown				IVS4 +5 G>A	2 (1)	Unknown
M520R	3 (2)	Unknown	Y281C	4 (1)	Unknown				R195fs/40	2 (1)	No‡
Q357H	3 (2)	Unknown	A226V	3 (1)	Unknown				K422fsX10	1 (1)	No‡
R360G	3 (2)	Unknown	A302V	3 (1)	Unknown				M1V	1 (1)	No‡

R583H	3 (2)	Unknown	G292D	3 (1)	Unknown						
S566F	3 (2)	Unknown	W305C	3 (1)	Unknown						
R562M	2 (1)	Unknown	E284K	2 (1)	Unknown						
W120C	2 (1)	Unknown	F296S	2 (1)	Unknown						
A525T	1 (1)	Unknown	G306R	2 (1)	Yes [11]						
G57V	1 (1)	Unknown	T322M	2 (1)	Unknown						
			V310I	2 (1)	Unknown						
			I274V	1 (0)	Unknown						
			P320H	1 (0)	Unknown						
			P343S	1 (0)	Yes [12]						
			R237P	1 (0)	Unknown						
			Y315S	1 (0)	Unknown						

*The biophysical function of the mutations was categorized as dominant-negative (>50% reduction in ion channel repolarizing current), haploinsufficiency (<50% reduction in ion channel repolarizing current), and unknown.
†Based on the present study.
‡Assumption based on the nature of the mutation.

Table 2S. Secondary confirmatory multivariate analyses: risk factors for aborted cardiac arrest or sudden cardiac death

A. Including the variable Cytoplasmic loops- missense vs. other mutations.

	Hazard ratio	**95% CI**	**P Value**
Gender/age			
Males age < 13 yrs	1.94	1.09-3.47	0.026
Females age 13 to 40 yrs	0.88	0.51-1.52	0.652
QTc ≥ 500 msec (vs. QTc<500)	3.46	1.80-6.63	<0.001
Cytoplasmic loops- missense vs. other mutations	2.74	1.68-4.46	<0.001

B. With adjustment for biophysical function

	Hazard ratio	**95% CI**	**P Value**
Gender/age			
Males age < 13 yrs	1.96	1.09-3.52	0.024
Females age 13 to 40 yrs	0.87	0.51-1.49	0.610
QTc ≥ 500 msec (vs. QTc<500)	3.46	1.79-6.70	0.000
Cytoplasmic loops- missense vs. other mutations	2.87	1.74-4.75	<0.001
Dominant negative vs. Haploinsufficiency.*	0.97	0.52-1.81	0.929

Adjusted also for unknown biophysical function.

* In a separate model adjusting only for biophysical function (including unknown function), Dominant negative vs. Haploinsufficiency HR= 2.15, 95% CI 1.15-4.02, p=0.017.

C. Excluding patients with V254M mutation.

	Hazard ratio	**95% CI**	**P Value**
Gender/age			
Males age < 13 yrs	2.14	1.09-4.24	0.028
Females age 13 to 40 yrs	0.70	0.40-1.22	0.207
QTc ≥ 500 msec (vs. QTc<500)	4.45	2.26-8.76	<0.001
Cytoplasmic loops- missense (excluding V254M) vs. other mutations	1.89	1.09-3.26	0.024

D. Including appropriate ICD shocks in the composite end point.

	Hazard ratio	**95% CI**	**P Value**
Gender/age			
Males age < 13 yrs	1.70	0.95-3.05	0.074
Females age 13 to 40 yrs	0.95	0.57-1.60	0.849
QTc ≥ 500 msec (vs. QTc<500)	3.26	1.75-6.09	<0.001
Cytoplasmic loops- missense vs. other mutations	2.64	1.65-4.23	<0.001

All tables adjusted also for time-dependent ß-blocker treatment and for QTc missing.

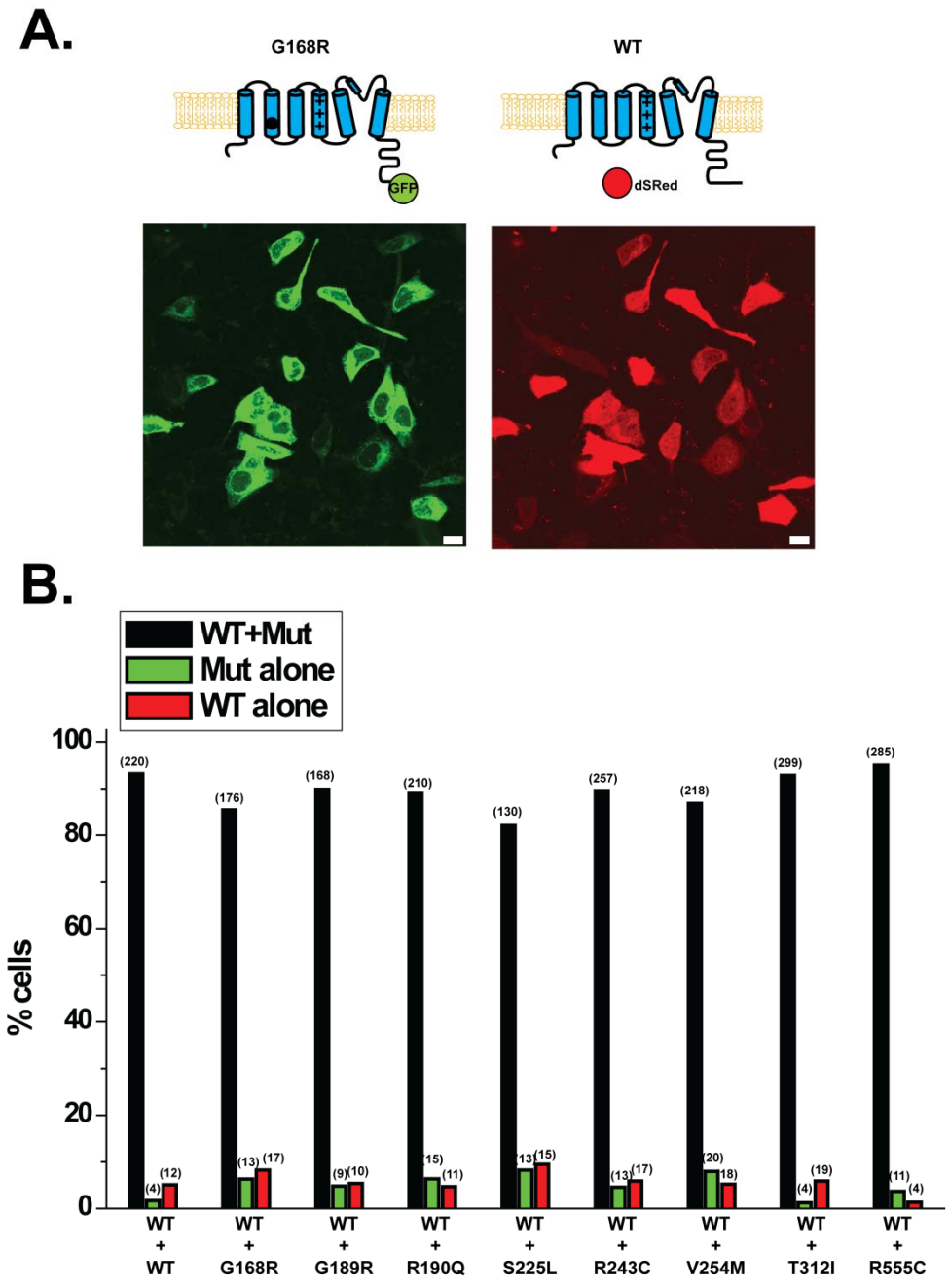

Supplementary Figure 1S.

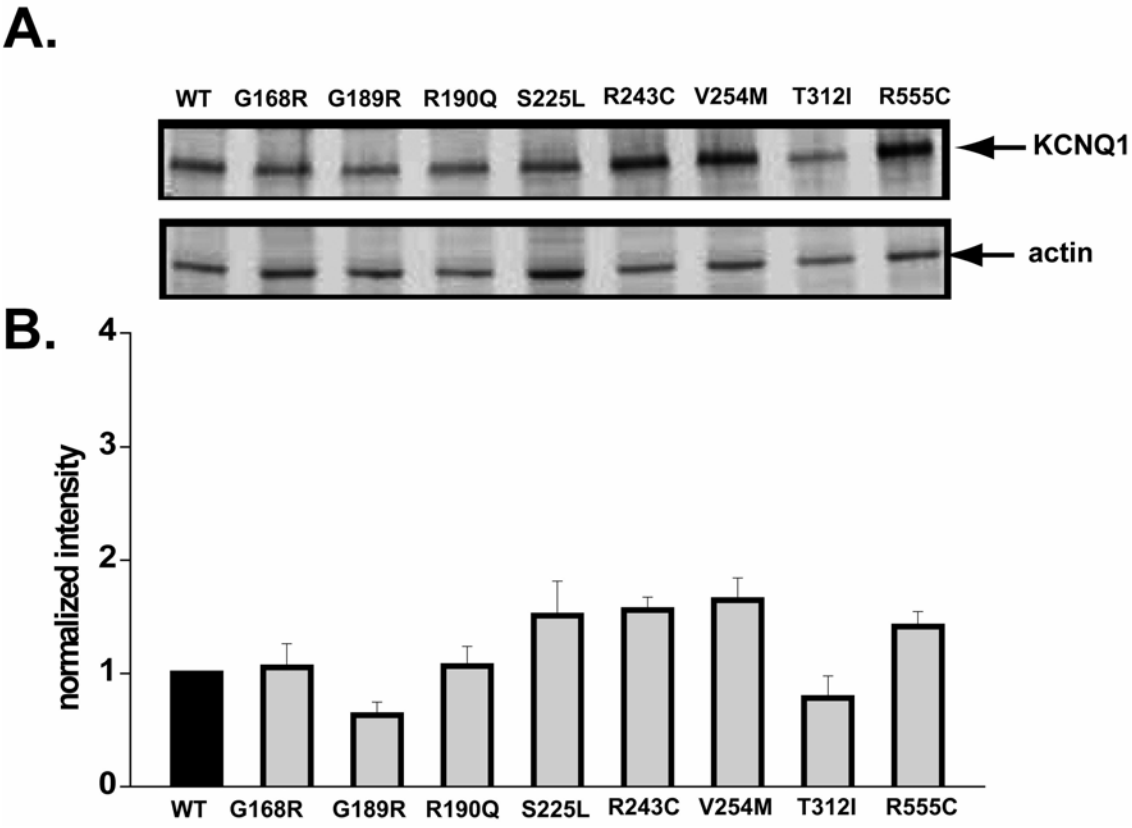

Supplementary Figure 2S.

Figure Legends

Supplementary Figure 1S. Co-expression of WT- and mutant-*KCNQ1* subunits in HEK293T cells.

A. Schematic pictures of the DNA constructs used for confirming co-expression of WT- and mutant-*KCNQ1* subunits in HEK293T cells. GFP was tagged to mutant *KCNQ1* at C-term (upper panel, left). WT-*KCNQ1* was introduced in pIRES2-DsRed plasmid containing unlinked *KCNQ1* and DsRed fluorescence cDNA (see also Supplementary Material and Methods) (upper panel, right). Each GFP-tagged mutant *KCNQ1* plasmid was transfected with WT *KCNQ1* in pIRES2-DsRed plasmid and *KCNE1* at the ratio of 0.5 μg mutant *KCNQ1*: 0.5 μg WT-*KCNQ1*: 1 μg *KCNE1* to mimic heterozygous mutation. Representative pictures obtained from confocal microscope shown in lower panels showed that most of the cells were expressing both WT-*KCNQ1* and *KCNQ1*(G168R) subunits. Scale bar in each panel, 10 μm. **B.** Summary data obtained from all mutants tested. WT channels expression (GFP-tagged WT-*KCNQ1*: WT-*KCNQ1* in pIRES2-DsRed plasmid: *KCNE1*= 0.5 μg :0.5 μg: 1μg) is shown as control experiments (showing as WT+WT). The number of the cells used for analysis is shown in parentheses. Untransfected cells show very low background green and red fluorescence compared to transfected cells (not shown).

Supplementary Figure 2S. Expression of WT- and mutant-*KCNQ1* subunit proteins in HEK293T cells.

Representative Western blotting picture for WT- and mutant-*KCNQ1* subunit proteins expressed in HEK293T cells. HEK293T cells were co-transfected with either WT- or

mutant *KCNQ1* (1 μg), in addition to *KCNE1* (1 μg) and pEGFP-N1 (0.2 μg). Lysates were subjected to 10% SDS-PAGE followed by immunoblotting with anti-*KCNQ1* antibody and anti-β-actin antibody. **B.** Summary data obtained from 4-9 experiments. The band intensity of each mutant subunit was not significantly changed compared to that of WT (G168R, p=1.00; G189R, p= 0.850; R190Q, P=1.00; S225L, P=0.492; R243C, P=0.309; V254M, P=0.222; T312I, P=0.994; R555C, 0.750). Normalized intensity was determined by measuring intensity of *KCNQ1* protein and β-actin protein in each lane to control for protein loading. *KCNQ1*/ β-actin ratio for each mutant was normalized to WT/ β-actin ratio in each blot.

Supplemental References

1. Loussouarn G, Baro I, Escande D. KCNQ1 K+ channel-mediated cardiac channelopathies. *Methods Mol Biol*. 2006;337:167-183
2. Vanoye CG, Welch RC, Daniels MA, Manderfield LJ, Tapper AR, Sanders CR, George AL, Jr. Distinct subdomains of the KCNQ S6 segment determine channel modulation by different KCNE subunits. *J Gen Physiol*. 2009;134:207-217
3. Jons C, J OU, Moss AJ, Reumann M, Rice JJ, Goldenberg I, Zareba W, Wilde AA, Shimizu W, Kanters JK, McNitt S, Hofman N, Robinson JL, Lopes CM. Use of mutant-specific ion channel characteristics for risk stratification of long QT syndrome patients. *Sci Transl Med*. 2011;3:76ra28
4. Williams DM, Lopes CM, Rosenhouse-Dantsker A, Connelly HL, Matavel A, J OU, McBeath E, Gray DA. Molecular basis of decreased Kir4.1 function in sesame/east syndrome. *J Am Soc Nephrol*. 2010;21:2117-2129
5. J OU, Komukai K, Kusakari Y, Obata T, Hongo K, Sasaki H, Kurihara S. Alpha1-adrenoceptor stimulation potentiates L-type Ca2+ current through Ca2+/calmodulin-dependent PK II (CaMKII) activation in rat ventricular myocytes. *Proc Natl Acad Sci U S A*. 2005;102:9400-9405
6. Jhun BS, J OU, Wang W, Ha CH, Zhao J, Kim JY, Wong C, Dirksen RT, Lopes CM, Jin ZG. Adrenergic signaling controls rgk-dependent trafficking of cardiac voltage-gated l-type Ca2+ channels through PKD1. *Circ Res*. 2012;110:59-70
7. Sanguinetti MC, Curran ME, Zou A, Shen J, Spector PS, Atkinson DL, Keating MT. Coassembly of K(V)LQT1 and minK (IsK) proteins to form cardiac i(ks) potassium channel. *Nature*. 1996;384:80-83
8. Chouabe C, Neyroud N, Guicheney P, Lazdunski M, Romey G, Barhanin J. Properties of KVLQT1 K+ channel mutations in Romano-Ward and Jervell and Lange-Nielsen inherited cardiac arrhythmias. *EMBO J*. 1997;16:5472-5479
9. Shalaby FY, Levesque PC, Yang WP, Little WA, Conder ML, Jenkins-West T, Blanar MA. Dominant-negative KVLQT1 mutations underlie the LQT1 form of long QT syndrome. *Circulation*. 1997;96:1733-1736
10. Kubota T, Shimizu W, Kamakura S, Horie M. Hypokalemia-induced long QT syndrome with an underlying novel missense mutation in S4-S5 linker of KCNQ1. *J Cardiovasc Electrophysiol*. 2000;11:1048-1054
11. Wang Z, Tristani-Firouzi M, Xu Q, Lin M, Keating MT, Sanguinetti MC. Functional effects of mutations in KVLQT1 that cause long QT syndrome. *J Cardiovasc Electrophysiol*. 1999;10:817-826
12. Zehelein J, Thomas D, Khalil M, Wimmer AB, Koenen M, Licka M, Wu K, Kiehn J, Brockmeier K, Kreye VA, Karle CA, Katus HA, Ulmer HE, Schoels W. Identification and characterisation of a novel KCNQ1 mutation in a family with Romano-Ward syndrome. *Biochim Biophys Acta*. 2004;1690:185-192